PAPER • **OPEN ACCESS**

Hydrophilic and hydrophobic shape memory polymer networks in high-intensity focused ultrasound fields

To cite this article: Jiaxin Xi *et al* 2024 *Smart Mater. Struct.* **33** 025024

OPEN ACCESS
IOP Publishing
Smart Materials and Structures
Smart Mater. Struct. **33** (2024) 025024 (10pp)
https://doi.org/10.1088/1361-665X/ad1d07

Hydrophilic and hydrophobic shape memory polymer networks in high-intensity focused ultrasound fields

Jiaxin Xi[1], **Ahmed Sallam**[1], **David L Safranski**[2,3], **Reza Mirzaeifar**[1,4] and **Shima Shahab**[1,*]

[1] Department of Mechanical Engineering, Virginia Tech, Blacksburg, VA 24061, United States of America
[2] Enovis Foot & Ankle, Atlanta, GA 30318, United States of America
[3] School of Materials Science and Engineering, Georgia Institute of Technology, Atlanta, GA 30332, United States of America

E-mail: sshahab@vt.edu

Received 12 May 2023, revised 5 December 2023
Accepted for publication 10 January 2024
Published 19 January 2024

Abstract

High-intensity focused ultrasound (HIFU) has been investigated as a remote and controlled activation method to noninvasively actuate shape memory polymers (SMPs), specifically in biomedical applications. However, the effects of aqueous environment on shape recoverability of *in vivo* HIFU-actuated SMPs have yet to be explored. HIFU directs sound waves into a millimeter-sized tightly focused region. In this study, the response of hydrophilic and hydrophobic photopolymerized thermoset SMP networks under HIFU activation in an aqueous environment was investigated. Acrylate-based SMP networks were copolymerized in specific ratios to produce networks with independently adjusted glass transition temperatures ranging from 40 to 80 °C and two distinct water uptake behaviors. The results link the polymer swelling behavior to shape recoverability in various acoustic fields. The presence of absorbed water molecules enhances the performance of SMPs in terms of their shape memory capabilities when activated by HIFU. Overall, understanding the interplay between water uptake and HIFU-actuated shape recovery is essential for optimizing the performance of SMPs in aqueous environments and advancing their use in various medical applications.

Supplementary material for this article is available online

Keywords: shape memory polymer (SMP), hydrophilic, hydrophobic, high-intensity focused ultrasound (HIFU)

[4] The authors wish to dedicate this work to the late Dr Reza Mirzaeifar (deceased 19 October 2022) of Virginia Tech.
[*] Author to whom any correspondence should be addressed.

1. Introduction

Shape memory polymers (SMPs) are a class of smart materials that have gained attention due to their potential use in a variety of medical fields, including tissue, stents, drug delivery systems, and orthopaedic devices [1–5], thanks to their exceptional benefits including lightweight, affordability, versatility, and ease of processing [6, 7]. The ability of SMPs to revert to their permanent shape after being subjected to an external stimulus, such as heat, solvent, pH, and a focused ultrasound (FU) field [8–15], is a key feature. The underlying mechanism for this shape memory effect is due to the internal transition from a glassy to a rubbery state or component softening/transition during the heating cycle [16]. The activation temperature range of SMPs, often related to the glass transition temperature (T_g), can be adjusted by modifying the copolymer composition or degree of crosslinking [17–20].

The shape memory effect in SMPs depends on an external stimulus, making the choice of activation method a crucial factor. Direct heating is one of the most widely used activation methods, owing to the benefits of easy control of the switching temperature, and excellent shape memory behaviors; however, its application *in vivo* is unfeasible due to the potential for irreversible tissue damage resulting from the higher activation temperature [21, 22]. In contrast, activation with body heat has been investigated to avoid thermal damage; however, precisely tuning the thermal transition temperature of SMPs is difficult, limiting their use in biomedical applications [23]. An alternative method, solvent-driven temperature SMP, has been proposed as a way to activate SMPs [10]. However, the choice of solvent can impact its performance and limit its use for *in vivo* applications, as some solvents are not suitable for use inside the body. Indirect activation methods, such as light [24, 25], magnetic fields [26, 27], electrical fields [28], and radio frequency waves [29], have emerged as promising options to overcome the aforementioned problems. Nevertheless, these activation methods have potential safety risks to the human body and may be inconvenient. For instance, magnetic SMPs must use magnetic particles that are non-toxic, biodegradable, and biocompatible to ensure safety in medical applications. As a result, finding a safer and more efficient activation method for remote shape recovery in SMPs is critical for their successful application in the biomedical field.

High-intensity focused ultrasound (HIFU) is an innovative and promising stimulus with a unique and superior capability to noninvasively achieve shape recovery by inducing localized heating and activating various intermediate forms [30–32]. There are four main steps in the shape recovery cycle. Step 1 involves heating the polymer above T_g before deforming it into the appropriate shape. Step 2 involves preserving the initial deformation constraint while cooling the polymer to a temperature below T_g. Step 3 involves releasing the deformation constraint and fixing the temporary shape. In step 4, once the temperature is raised above T_g, the polymer returns to its initial (permanent) structure. Stages 1–3 are also known as the programming stages. Depending on whether or not the external loads still persist, that is, the constrained or free recovery state [33], the SMP could either provide recovery stresses or return to their permanent shapes when an external stimulus (in our case, HIFU) is delivered in step 4. The final state of the material in this study's SMPs recovery process (step 4) is stress-free, and the heating of the polymer is caused by the absorption of acoustic energy as a result of the viscous shearing applied by ultrasonic focused waves and subsequent release of energy in the form of heat [34]. By concentrating sound waves into a millimeter-scale area, where they interact with polymer chains to produce localized heating while sparing the surrounding area, HIFU provides selective and controlled heating. Mechanical waves are triggered by HIFU through the polymer matrix, which results in viscous shearing and relaxation, which results in damping losses [35]. Additionally, internal friction and energy absorption occur during HIFU exposure as a result of viscoelastic polymeric materials' strain lagging behind their stress. A portion of this energy is transformed into heat during the first stage of its absorption, and the remaining energy is stored as an elastic deformation in the polymer chains during the second step. The temperature of the polymer rises as a result of internal friction that transforms ultrasonic energy into heat [34]. Then, just like with free recovery, that heat starts the form recovery process. As a result, HIFU represents a practical option for activation biomedical SMPs. HIFU activation of SMPs has been reported for biomedical applications such as drug delivery and drug release [14, 31, 32], which involve the activation of SMPs within the human body by exposing the SMPs to water in biological aqueous environment, such as blood vessels. To the authors' best knowledge, previous studies have focused on the optimization of SMP compositions; it has not been thoroughly studied how an aqueous environment affects a HIFU-actuated SMP's capacity to regain its original shape. It is hypothesized that when SMPs are subjected to HIFU in an aqueous environment, their heating behavior differs from that of direct exposure to HIFU; however, the causes for this divergence remain entirely unknown. This study aims to close this gap by investigating how water uptake affects the shape memory behavior of SMPs in various HIFU fields.

In this study, we propose that shape memory performance can be enhanced by varying the concentration of acrylate-based polymers with varying glass transition temperatures and water uptake behaviors. The biocompatibility of acrylate-based SMPs positions them as promising candidates for various biomedical applications [36, 37]. We specifically created six acrylate copolymers with two different water uptake behaviors (hydrophilic and hydrophobic) and three glass transition temperatures (40, 60, and 80 °C). Dynamic mechanical analysis (DMA) is used to characterize the SMP's thermal properties. This is similar to the illustration in figure 1, and bend recovery testing is used to assess the shape memory behavior with HIFU as the stimulus.

2. Materials and methods

2.1. Sample preparation

Six acrylate copolymers with glass transition temperatures of 40, 60, and 80 °C and two distinct water uptake behaviors

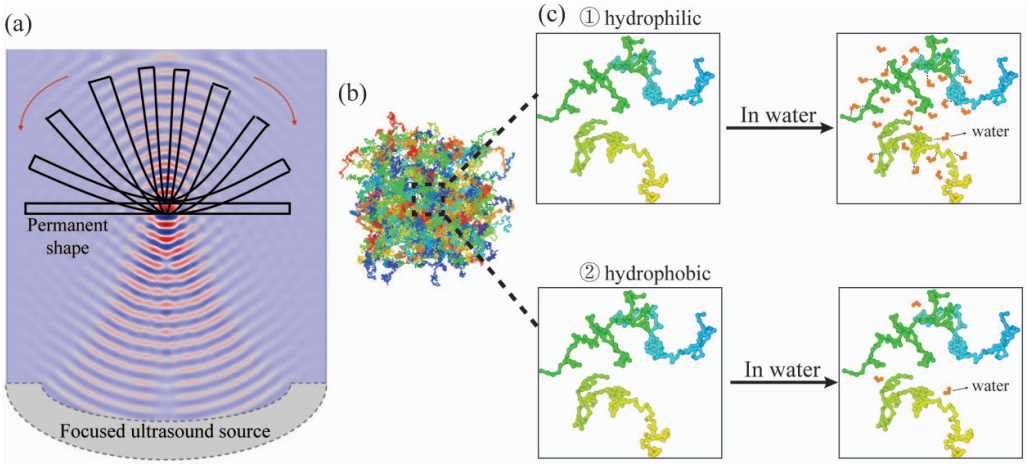

Figure 1. (a) Schematic of acoustic wave from a focused ultrasound source to a shape memory polymer specimen. Schematic representations of (b) SMP chain system and (c) swelling process of ① Hydrophilic polymer and ② Hydrophobic polymer. The dashed black line represents hydrogen bonds for respective water molecules. The orange atoms are water molecules.

Table 1. SMP compositions.

Fixed Mol Percent of 5.0 CN9009 for Polymer networks		
Sample code		
Copolymer 1	35 mol% Isobornyl acrylate	60 mol% Butyl acrylate
Copolymer 2	95 mol% 2-hydroxyethyl acrylate	
Copolymer 3	50 mol% Isobornyl acrylate	45 mol% Butyl acrylate
Copolymer 4	10 mol% Poly(ethylene glycol) diacrylate	85 mol% 2-hydroxyethyl methacrylate
Copolymer 5	70 mol% Isobornyl acrylate	25 mol% Butyl acrylate
Copolymer 6	45 mol% 2-hydroxyethyl acrylate	50 mol% 2-hydroxyethyl methacrylate

(hydrophilic and hydrophobic) were synthesized. Aliphatic urethane-acrylate oligomer (CN9009, MW∼1860) was supplied by Sartomer Inc. (Exton, PA). Isobornyl acrylate (IBA), 2-hydroxyethyl acrylate (2-HEA), poly(ethylene glycol) diacrylate (PEGDA, MW = 700), butyl acrylate (BA), 2-hydroxyethyl methacrylate (HEMA) and the photoinitiator 2,2-Dimethoxy-2-phenylacetophenone (DMPA) were purchased from Sigma-Aldrich, Inc. and used as received without further purification. Figure 2(a) illustrates the SMP mixtures preparation procedure. Table 1 describes polymer networks with a fixed 5.0 mole percent (mol%) CN9009. In the experiment, each polymer network was first mixed as shown in table 1, followed by 0.5 weight percent (wt%) photoinitiator DMPA added into the solution. The solution was then fully stirred for 20 min. Afterwards, the polymer solution was injected into a mold composed of two glass slides separated by 1- or 2 mm silicone rubber spacers. Glass slides were first coated with Rain-X as a mold release agent. The injected molds were then polymerized for 30 min using an ultraviolet crosslinker (UVP CL-1000). The prepared SMP mixtures were post-cured and dried inside the fume hood for 24 h.

Due to the variety of prepared specimens, a straightforward nomenclature was developed. Samples were labeled as CN9009, depending on the main crosslinker. For those named CN9009_T# (e.g. 40, 60 or 80)_Q*(e.g. 1 or 2), T(#) represents the glass transition temperature, Q(*) represents the swelling behavior (Q1 represents hydrophobic, and Q2 represents hydrophilic).

2.2. Material characterization

To compare the equilibrium swelling ratio of each SMP mixture, it was evaluated under ASTM D570 [38]. The sample was cut into 10 mm × 10 mm × 1 mm square-shaped film. Using a digital balance with a resolution of 10–4 gram (A&D GR-202), each specimen was weighed before testing and after 24 h in a large amount of water. Specimens were also removed and weighed at fixed intervals to calculate the swelling ratio. To ensure the repeatability, for the material set in table 1, each composition was tested at least four times ($n = 4$). Here, the swelling ratio (S_w) is defined as the difference between the initial dry weight (m_0) and the equilibrium weight (m_{eq}) divided by the initial dry weight of specimen ($S_w\,(\%) = \frac{m_{eq}-m_0}{m_0} \times 100$). The swelling ratio of each material set was averaged from four pieces of samples, and the error bars represented the standard deviations.

Crank [39] developed equations for specific geometries to solve Fick's law. Those include an equation describing diffusion into a planar sheet, which also has been used in other studies [33, 40–44]. To compare the diffusion coefficients of

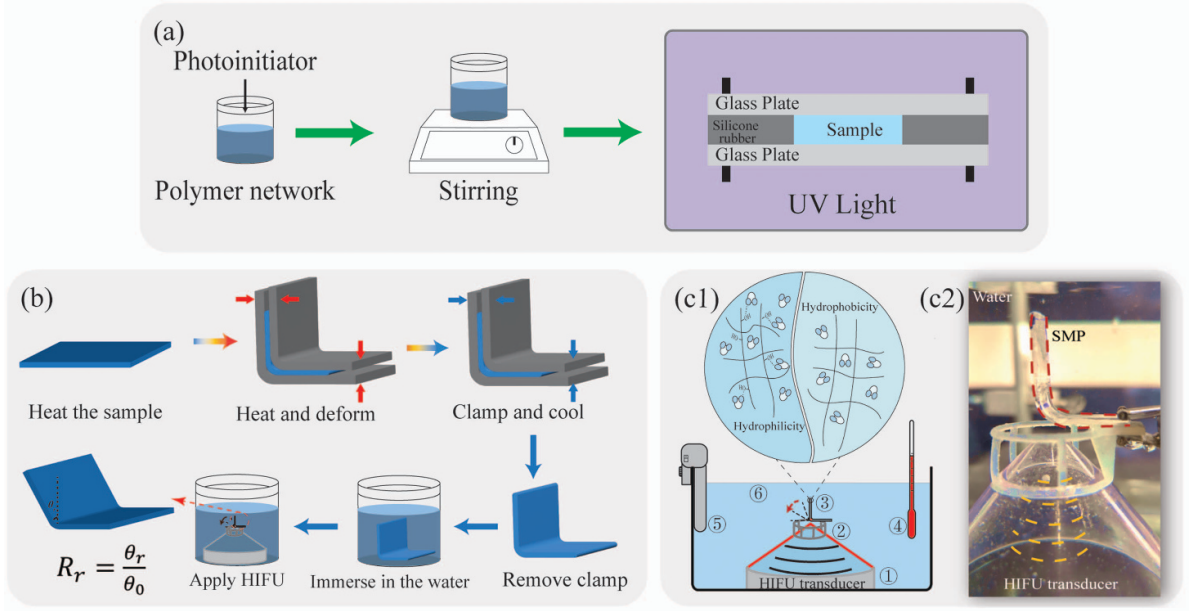

Figure 2. (a) Schematic diagram of the fabrication steps of SMP mixtures. (b) Schematic diagram of the test procedure for characterizing shape recovery by bending test method. (c1) Illustration of the experimental setup; ① the HIFU transducer placed on the bottom of the tank; ② custom 3D-printed sample holder; ③ shape memory polymer filament; ④ thermometer; ⑤ immersion tank heater; ⑥ water bath. (c2) Experimental HIFU setup.

each hydrophilic network, the following equation (1) for diffusion into a plane sheet [45] was considered:

$$\frac{M_t}{M_\infty} = 1 - \sum_{n=0}^{\infty} \frac{8}{(2n+1)^2 \pi^2} \exp\left[-\frac{D(2n+1)^2 \pi^2 t}{4l^2}\right]. \quad (1)$$

At early stages and small times, the diffusion process is calculated as

$$\frac{M_t}{M_\infty} = 2\left(\frac{Dt}{\pi l^2}\right)^{\frac{1}{2}} \quad (2)$$

where M_t is the mass of water at time t, M_∞ is the mass of water at equilibrium state, l is the thickness of sheets, and D is the diffusion coefficient. In this case, one-dimensional diffusion is assumed because, in a sufficiently thin plane sheet, the majority of the diffusing substance enters through the faces while only a trace enters through the edges.

To characterize the temperature-dependent storage modulus, loss modulus, and tan delta, DMA was performed as per ASTM D4065 and D4440 [46, 47] using a TA-Q800 DMA tester (TA Instruments). The test was performed in DMA's dynamic mode at 1 Hz frequency. Samples were prepared by scissor cutting specimens to 20 mm × 5 mm × 1 mm from bulk material. The specimen was equilibrated at 25 °C for 20 min before being heated to 110 °C at 5 °C min^{-1} with 0.1% dynamic strain, 0.001 N preload force, and 150% force track. To ensure the repeatability, each composition was tested at least three times ($n = 3$).

2.3. SMP-HIFU experiments: shape recovery analysis

Figure 2(c1) depicts the HIFU system's configuration. A HIFU transducer and a sample-holder module were the two main parts. The bottom of a water-filled tank housed the H-104-4A SONIC Concepts HIFU transducer. The body temperature (37 °C) was reached and maintained by heating the water in the tank. The ultrasound frequency was 500 kHz. Recovery tests were carried out on flat 50 mm × 5 mm × 2 mm film specimens. Schematic diagram of the test procedure for characterizing shape memory behavior is described in figure 2(b). Prior to folding into an L shape ($\theta_0 = 90°$) for 10 min, the specimen was first heated above the glass transition temperature in an oven for 10 min. The specimen was then cooled while clamped. Then the external force was removed. Afterwards, two methods were used to actuate the SMP mixtures. On the one hand, in order to investigate the recovery in water with no HIFU activation, the bent specimen was unmounted and immersed in warm water at body temperature after unmounted. On the other hand, for recovery under HIFU with water treatment, the specimen was first immersed in warm water for 0, 1, 2, or 3 min (CN9009_T60_Q2), or 0, 10, 20, or 30 min (CN9009_T80_Q2); and then, HIFU thermally actuated the specimen. It is noted that the sample bend had to be located on the focal point of the FU transducer, as shown in figures 2(c1) and (c2). The momentary shape was recorded using a digital camera in the whole recovery process; and then Kinovea (version 0.9.5, an open-source project) was used to process the video [48] and output recovery angles (θ_r) at fixed intervals. The recovery ratio (R_r) was defined as the ratio between the recovered angle (θ_r) and the opening

angle (θ_0) when heated. To reduce the experimental error, at least six runs in one set for each sample were conducted (n =6).

3. Results and discussion

3.1. Synthesis and thermo-mechanical characterization of polymer networks

The purpose of this study was to develop SMPs, which exhibit shape-memory behavior in FU field relevant to biomedical applications. Thermal transitions play an important role in the design and application of thermally responsive SMPs. It is important to note that the glass transition temperature of HIFU-actuated biomedical SMPs should be higher than the body temperature for those SMPs to maintain an intermediate shape and recover to their permanent shape at the targeted location. To accomplish this, the linear equation [49], $T_g = w_1 T_{g1} + w_2 T_{g2}$, was used to predict the glass transition temperature (T_g) of SMP copolymers, where T_{g1} and T_{g2} are the glass transition temperatures of homopolymers A and B, and w_1 and w_2 are the weight percentages, respectively. Furthermore, to determine the shape memory behavior of each hydrophilic and hydrophobic SMPs with the same T_g, hydrophilic 2-HEA, PEGDA, and HEMA and hydrophobic IBA and BA were introduced into SMP networks. T_g was calculated using DMA and the peak of tan delta, as shown in the Supplementary information. The equilibrium swelling ratio of the SMP networks was determined using the method described in section 2.2. Figure 3(a) shows the glass transition temperatures and swelling ratios of six different acrylate copolymer networks that were used in all of the subsequent experiments in this study. The highest swelling ratios were 29.27 ± 0.74%, 29.43 ± 0.41%, and 26.89 ± 0.10% at 40, 60, and 80 °C, respectively, while the lowest swelling ratios were 0.93 ± 0.19%, 4.28 ± 0.26%, and 1.37 ± 1.41%.

Figures 3(b) and (c) show the normalized swelling ratio of hydrophobic and hydrophilic SMP networks as a function of the square root of time, respectively. The hydrophobic copolymers with no obvious variation showed that the copolymers were relatively stable, as shown in figure 3(b), whereas the swelling ratio of hydrophilic copolymers showed an upward trend as immersion time increases, as shown in figure 3(c). Water molecules penetrate into the crosslinking networks, interacting physically and/or chemically until they reach equilibrium. Figure 3(c) shows that the hydrophilic networks remained linear for up to 24 h, implying Fickian diffusion. The experimental data were numerically fitted to the Fickian equation to quantify diffusion, yielding diffusion coefficients of 4.25 × 10^{-11}, 3.51 × 10^{-11}, and 2.49 × 10^{-11} $m^2 s^{-1}$ for hydrophilic networks with glass transition temperatures of 40, 60, and 80 °C, respectively. At the same solution temperature, the results showed that a higher glass transition temperature is associated with a lower diffusion coefficient. This is because higher glass transition temperatures result in tighter packing of polymer chains, resulting in limited mobility and impeding the movement of diffusing species through the polymer matrix [50]. As a result, at higher glass transition temperatures, the diffusion coefficient is lower.

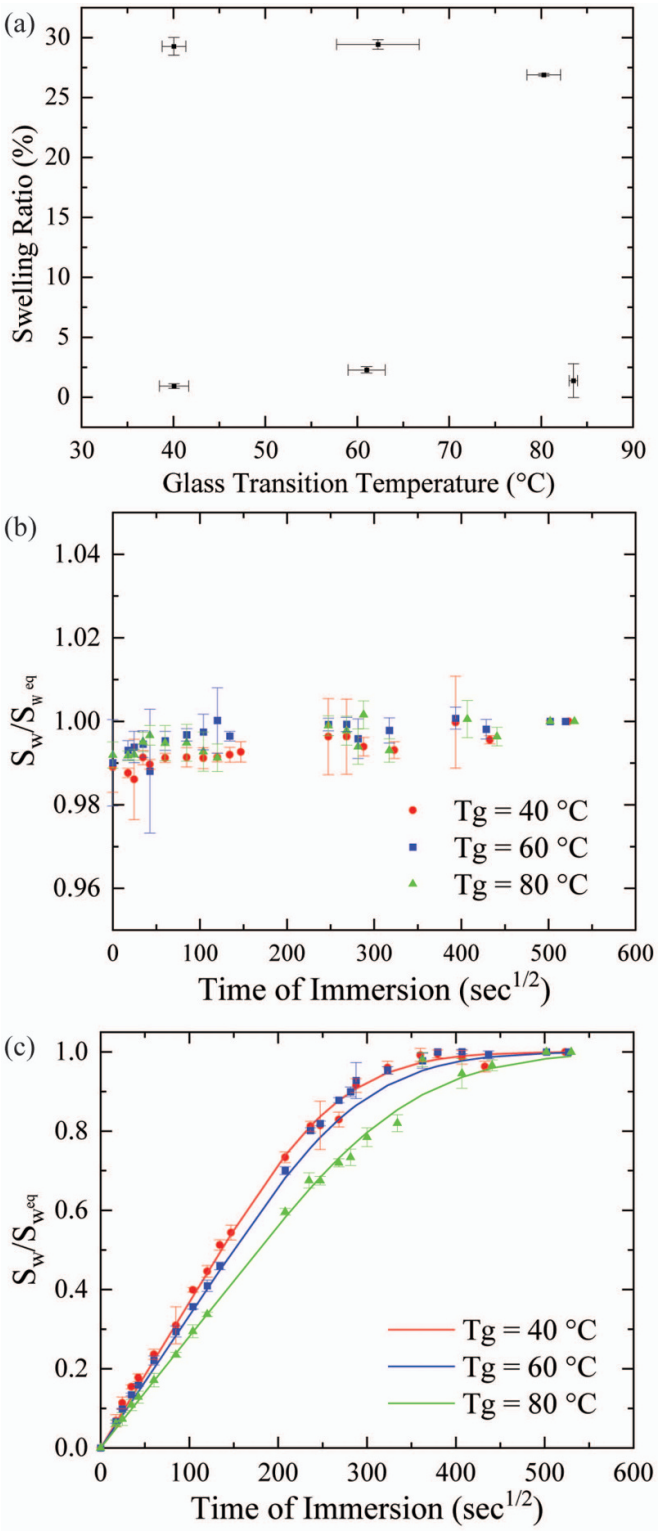

Figure 3. (a) Swelling ratio vs. Glass transition temperature for each polymer network. Swelling rate of (b) hydrophobic and (c) hydrophilic materials, with the T_g of 40 °C (red), 60 °C (blue), and 80 °C (green). Point is experimental data; line is theoretical fit based on Fickian diffusion.

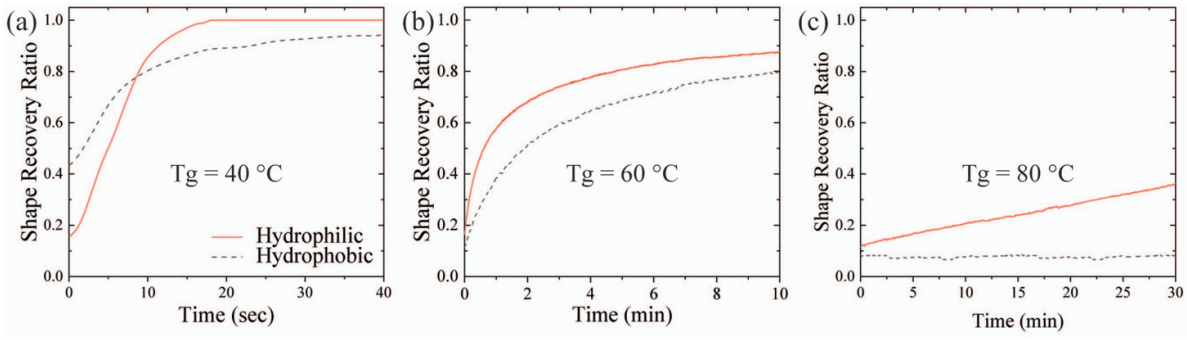

Figure 4. Recovery performance of specimens in warm water for both hydrophobic and hydrophilic materials with the (a) $T_g = 40$ °C, (b) $T_g = 60$ °C and (c) $T_g = 80$ °C.

3.2. Water-actuated shape memory effect

The shape recovery ratio as a function of time was characterized to determine the potential for shape memory performance. The water-driven shape memory recovery was first investigated because SMPs were exposed to water under HIFU activation. Figure 4 depicts the recovery performance of programmed SMP networks in warm water (∼37 °C). The recovery behavior was heavily influenced by the glass transition temperature and water uptake behavior. Figure 4(a) shows that CN9009_T40_Q2 recovered completely after 40 s in warm water, whereas CN9009_T40_Q1 recovered only partially. Because CN9009_T60_Q1 and CN9009 T60 Q2 presented a broad glass transition from 35 °C to 90 °C (see figures S1(c) and (d)), they had noticeable changes in warm water for the first 10 min. Figures S1(e) and (f) show that CN9009_T80_Q1 and CN9009_T80_Q2 exhibited a wide glass transition from 60 °C to 120 °C. The CN9009_T80_Q1 had no obvious shape recovery in warm water for the first 30 min, whereas the CN9009_T80_Q2 had a recovery ratio of 36% in warm water for the first 30 min. These findings indicate that the CN9009_T80 networks were relatively stable at body temperature. According to figure 4, hydrophilic SMPs recovered faster than hydrophobic ones.

The experimental findings indicated that both heat and water effectively activated SMPs. Moreover, when heat and water were applied in conjunction, the activation process was expedited, leading to a faster speed of shape recovery. The following are the reasons for this phenomenon. Water absorption leads to a reduction in the glass transition temperature (T_g) of SMPs. As plasticizers, water molecules penetrate the polymer matrix, retaining their mobility and forming hydrogen-bond clusters, known as 'free water' [51–54]. Although free water does not directly bond with the polymer network, it does influence its T_g, especially in the case of more hydrophobic polymers [51, 55]. This is accomplished by increasing the distance between polymer chains, thereby disrupting secondary bonding between chains, including hydrogen bonding and hydrophobic interactions. As a result, the polymer chains' flexibility and mobility are increased. As shown in figure 1(c), the hydrophilic copolymer has a greater number of polar side groups (hydroxyl groups (–OH)) than the hydrophobic material, which promotes hydrogen bonding between hydroxyl groups and water molecules, as the term 'bond water' [51–54, 56]. It is important to note that polymer chains carry no ionic charges during immersion. As reported by Miller [57], pHEMA lacks ionizing properties and that the 5 mol% crosslinker utilized severely restricts any charge carrier mobility. Previous studies [51, 52] have also examined similar methacrylate polymer systems and their interaction with water. Additionally, the hydroxyl groups in HEA and HEMA monomers are strongly bound to the monomer structure through covalent bonds and are resistant to hydrolysis or detachment by water [58, 59]. The T_g is influenced by bond water, because when water molecules form hydrogen bonds with polymer chains, a one-phase thermodynamic system is created, in which T_g is influenced by the concentrations of both the polymer network and water. As the weight fraction of bound water increases, the T_g steadily decreases [60–62], resulting in recovery process at a lower temperature. Previously, Xiao and Nguyen [63] proposed a constitutive model to investigate the influence of solvent absorption on the thermomechanical properties and shape-memory behavior of amorphous networks, based on Adam–Gibbs model [64]. According to the fundamental principles of the Adam–Gibbs theory [64], the relaxation time (or viscosity) exhibits an inverse correlation with configurational entropy. When solvent permeates the polymer matrix, there is a rise in configurational entropy owing to the blending of solvent and polymer segments [65]. T_g can be measured using dynamic frequency sweep tests or differential scanning calorimetry on dry and saturated specimens in this case [63, 64]. However, these two methods are ineffective in this study because, after being immersed in water for up to 40 s (CN9009_T40), 10 min (CN9009_T60), or 30 min (CN9009_T80), the swollen specimen dries in air in less than 1 min. Environmental DMA is recommended to analyze T_g, but it is challenging to access for the current study because specimens must be completely submerged in water. Previous research [10, 60–62, 66, 67] has demonstrated how water can alter T_g. Uthaman *et al* [60] investigated the effect of water on the aging of epoxy resin and carbon fiber-reinforced polymer composites and discovered that the glass transition temperature of both neat epoxy resin and composites decreased in water at body temperature, similar to tensile

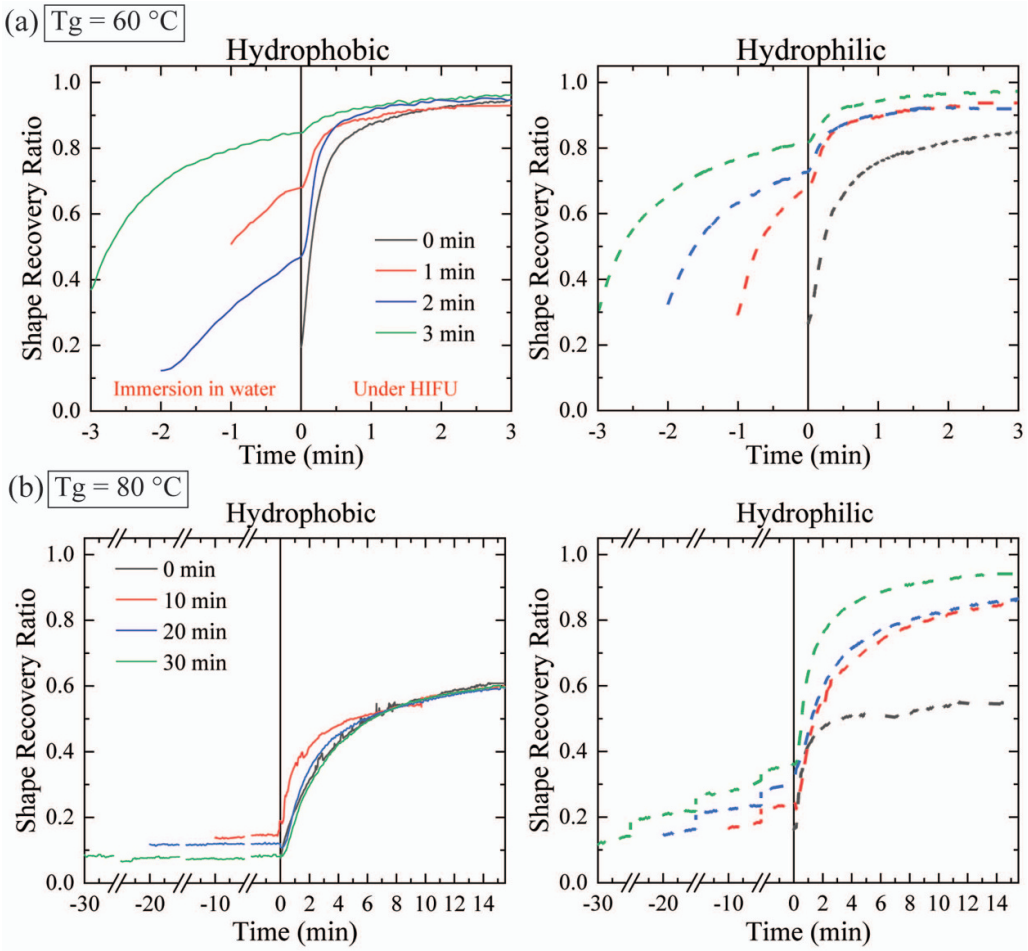

Figure 5. Shape recovery ratio for SME with the (a) $T_g = 60$ °C, (b) $T_g = 80$ °C, shown as a function of time with pre-immersion treatment and under HIFU activation.

strength and moduli. According to Yang *et al* [68], the T_g of polyurethane SMPs drops sharply from 37 to 6 °C within the first 162 h of immersion, followed by a gradual decrease. The study offers valuable insights into the mechanisms that impact shape memory performance, paving the way for optimizing the activation of SMP systems through a combination of water immersion and direct heat.

3.3. HIFU actuated shape memory effect

As shown in the previous section, SMPs with glass transition temperature of 60 °C and 80 °C recovered very slow in water at body temperature. Therefore, HIFU was applied to activate the shape memory process. HIFU-actuated shape recovery was investigated by immersing the sample in the HIFU reactor's water bath at 37 °C. Figure 5 depicts the recovery performances of programmed CN9009_T60_Q1, CN9009_T60_Q2, CN9009_T80_Q1, and CN9009_T80_Q2 films after immersion in water for varying lengths of time. Figure 5 shows that increasing the immersion time from 0 to 1, or 2, or 3 min improved the shape recovery ratio of CN9009_T60_Q2 from 85% to 92% and 97%, respectively. Similarly, as the immersion time for CN9009_T80_Q2 increased from 0 to 10, or 20, or 30 min, the shape recovery ratio increased from 55% to 87% and 95%. However, after pre-treatment, there was no discernible difference in the hydrophobic SMPs' synergistic HIFU-actuated shape memory performance.

These findings proved that HIFU was a successful activation technique for SMPs. The concentrated application of HIFU on a specific spot induces a remarkable thermal effect on SMP materials. This is attributed to the ability of the polymer matrix to absorb acoustic energy generated by viscous shearing from the focused mechanical waves of HIFU, subsequently releasing this energy in the form of heat. Bhargava *et al* [13, 31, 32, 69] acoustic-thermoelastic mathematical framework for modeling the FU-induced thermal actuation of (SMPs), using Khokhlov–Zabolotskaya–Kuznetsov equation [70, 71]. When actuated with HIFU, the effects of acoustic nonlinearity on the induced thermal field in polymer, resulting in shape recovery. Furthermore, it was found that submerging hydrophilic SMPs in water prior to HIFU activation (referred to as per-immersion in the sections that follow for convenience) improved recovery performance in comparison to earlier studies. For instance, Bhargava *et al* [13] demonstrated that adjusting the composition ratio could increase the shape recovery ratio following a 20 s continuous ultrasonic exposure. The maximum recovery ratio was 20%, though. Peng *et al* [8] introduced polystyrene (PS) into SMP networks to optimize the recovery ratio; this

material exhibited almost 100% shape recovery in 2 s when direct heat was applied. Because PS increased viscoelasticity, they also proposed that adding it to the SMP network might improve the material's capacity to recover after exposure to HIFU. Pre-immersion hydrophilic SMPs provided an alternative mechanism in this study that demonstrated a notable improvement in shape recovery ability when activated by HIFU with energy savings. However, hydrophilic SMPs with pre-immersion exhibited the drawback of prior activation, rendering them unsuitable for biomedical applications. In contrast, hydrophobic copolymers displayed distinct advantages as their behavior remained unaffected by pre-immersion. This characteristic provided greater tailorability, albeit at the expense of requiring higher HIFU power and precise adjustment of T_g. Overall, optimizing the water absorption behavior of SMP copolymers allows for specific tailoring of their properties, particularly for biomedical applications.

The following explanation is put forth as a potential explanation for the aforementioned phenomena: During pre-immersion in water, the polymer absorbs water and softens as a result of the increased mobility of the polymer chains. The water-driven mechanism also lowers the temperature at which the SMPs become activated and raises viscoelasticity while lowering the tensile strength, tensile moduli, and elastic modulus. This means that even a lower-level acoustic power can easily reach the activation temperature and avoid any unpredictable damage inside the polymer, leading to easier activation of the SMP system. However, due to the limitations of thermal cameras, which are not suitable for analyzing submerged objects, the temperature increase within the interior of the polymer mixture was not measured in our case. Notely, the water's temperature was constant due to the precision of HIFU, which concentrates its energy on a millimeter-scale area. The interaction with polymer chains in this localized region results in specific heating, while the surrounding areas remain unaffected. In our previous work [13, 15, 31, 72], a 95% tert-butyl acrylate-5% di(ethylene glycol)dimethacrylate SMP specimen was suspended at the water's surface and subjected to HIFU, yielding a maximum temperature of 112.6 °C after 18 s [13]. Nonetheless, accurately determining the temperature of a specimen in water remains a challenge, and in the future, reliable temperature determination methodologies will be a focus of ongoing research.

It should be noted that the improved viscoelasticity of the SMP improves the efficiency of the HIFU thermal effect. Peng *et al* [73] found that the HIFU-actuated thermal effect of polymers is highly linked to material viscoelasticity. The viscous damping caused by the HIFU produces a noticeable thermal differential. According to their computational work, when viscoelastic amorphous polymers are subjected to HIFU, more heat is generated than that in crystalline polymers. Furthermore, the effect of ultrasound is altered after water absorption into the polymer. When ultrasound waves are emitted from the transducer surface to the polymer sample, some of the energy is reflected at the water-polymer interface, while the rest is transmitted through the polymer sample. The two materials' specific acoustic impedance ratio determines the transmitted energy fraction. The higher the transmission of acoustic energy through the polymer, the closer the acoustic impedance of the two materials is (i.e. the acoustic impedance ratio approaches unity). The swelling of a large amount of water is observed to bring the acoustical properties of hydrophilic polymers closer to those of water. Because the acoustic mismatch between water and the polymer interface is small, HIFU has a greater heating effect on the polymer. Consequently, the swelling behavior of hydrophilic SMPs improves their shape recovery ability. A similar phenomenon was reported in previous studies. Parker *et al* [74] reported that ethanol acts as a plasticizer on lactic and glycolic acid copolymers (PLGA) and has a significant impact on their acoustics. After 24 h in ethanal, the speed of sound on PLGA was reduced by approximately 10%, resulting in a significant decrease in the elastic modulus. Overall, the study provides insights into the mechanisms influencing shape memory performance and opens avenues for optimizing the activation of SMP systems using a combination of water immersion and HIFU.

4. Conclusions

The use of hydrophilic and hydrophobic photopolymerized thermoset acylate-based SMP networks and the relationship between polymer swelling behavior and shape recovery behavior in various acoustic fields have both been reported in this work. By varying copolymer composition, six acrylate-based SMP networks with glass transition temperatures of 40, 60, and 80 °C and two distinct water uptake behaviors (hydrophilic and hydrophobic) were created. In the polymer networks, shape memory recovery activated by water and HIFU was observed. Pre-immersion treatment improved the shape recovery ability of hydrophilic SMPs, but there was no discernible difference in the synergistic HIFU-actuated shape memory performance of hydrophobic SMPs. Because of the plasticizing effect of the water molecules, which occurred when water entered networks, the mobility of the polymer chains was increased. This resulted in the water-actuated shape recovery; in addition, the flexibility of the polymer chains indicates the high viscoelasticity and reduces the acoustic mismatch between water and the polymer interface, which leads to better heating of the polymer. Overall, these results show that hydrophilic and hydrophobic SMPs are a promising material for SMP-based biomedical devices, and the interaction between water uptake and HIFU-actuated shape recovery opens up the possibility of deciphering the mechanism and improving the design of SMP devices used in aqueous environments.

Data availability statement

The data cannot be made publicly available upon publication because no suitable repository exists for hosting data in this field of study. The data that support the findings of this study are available upon reasonable request from the authors.

Acknowledgments

This work was supported by the U.S. National Science Foundation (NSF) under Award No. CMMI 2016474, which is gratefully acknowledged.

Conflict of interest

The authors declare that they have no known competing financial interests or personal relationships that could have appeared to influence the work reported in this paper

ORCID iDs

Reza Mirzaeifar https://orcid.org/0000-0003-3427-0714
Shima Shahab https://orcid.org/0000-0003-1970-5345

References

[1] Delaey J, Dubruel P and Van Vlierberghe S 2020 Shape-memory polymers for biomedical applications *Adv. Funct. Mater.* **30** 1909047
[2] Xu L, Liu Y, Zhou W and Yu D 2022 Electrospun medical sutures for wound healing: a review *Polymers* **14** 1637
[3] de Melo Morgado G F, de Moura N K, Martins E F, Escanio C A, Backes E H, Marini J and Passador F R 2022 Effect of blend ratio on thermal, mechanical, and shape memory properties of poly (lactic acid)/thermoplastic polyurethane bio-blends *J. Polym. Res.* **29** 533
[4] Smith K E, Garcia M, Dupont K M, Higgs G B, Gall K and Safranski D L 2017 Shape-memory polymers for orthopaedic soft-tissue repair *Oper. Tech. Orthop.* **32** 141–8
[5] Ramaraju H, Akman R E, Safranski D L and Hollister S J 2020 Designing biodegradable shape memory polymers for tissue repair *Adv. Funct. Mater.* **30** 2002014
[6] Zhao Y, Peng K, Xi J, Shahab S and Mirzaeifar R 2022 Achieving multimodal locomotion by a crosslinked poly(ethylene-co-vinyl acetate)-based two-way shape memory polymer *Smart Mater. Struct.* **31** 015034
[7] Xing S-T, Wang P-P, Liu S-Q, Xu Y-H, Zheng R-M, Deng Z-F, Peng Z-F, Li J-Y, Wu Y-Y and Liu L 2020 A shape-memory soft actuator integrated with reversible electric/moisture actuating and strain sensing *Compos. Sci. Technol.* **193** 108133
[8] Peng K, Zhao Y, Shahab S and Mirzaeifar R 2020 Ductile shape-memory polymer composite with enhanced shape recovery ability *ACS Appl. Mater. Interfaces* **12** 58295–300
[9] Xi J, Shahab S and Mirzaeifar R 2022 Qualifying the contribution of fiber diameter on the acrylate-based electrospun shape memory polymer nano/microfiber properties *RSC Adv.* **12** 29162–9
[10] Xiao R, Guo J, Safranski D L and Nguyen T D 2015 Solvent-driven temperature memory and multiple shape memory effects *Soft Matter* **11** 3977–85
[11] Chi Y, Li Y, Zhao Y, Hong Y, Tang Y and Yin J 2022 Bistable and multistable actuators for soft robots: structures, materials, and functionalities *Adv. Mater.* **34** 2110384
[12] Cai Y, Jiang J-S, Liu Z-W, Zeng Y and Zhang W-G 2013 Magnetically-sensitive shape memory polyurethane composites crosslinked with multi-walled carbon nanotubes *Composites* A **53** 16–23
[13] Bhargava A, Peng K, Stieg J, Mirzaeifar R and Shahab S 2017 Focused ultrasound actuation of shape memory polymers; acoustic-thermoelastic modeling and testing *RSC Adv.* **7** 45452–69
[14] Bhargava A, Peng K, Mirzaeifar R and Shahab S 2018 Ultrasound actuated shape-memory polymer based drug delivery containers *Proc. SPIE* **10595** 105952H
[15] Bhargava A and Shahab S 2019 Coupling of nonlinear shape memory polymer cantilever dynamics with focused ultrasound field *Smart Mater. Struct.* **28** 055002
[16] Huang W M, Zhao Y, Wang C C, Ding Z, Purnawali H, Tang C and Zhang J L 2012 Thermo/chemo-responsive shape memory effect in polymers: a sketch of working mechanisms, fundamentals and optimization *J. Polym. Res.* **19** 9952
[17] Xiao X, Kong D, Qiu X, Zhang W, Zhang F, Liu L, Liu Y, Zhang S, Hu Y and Leng J 2015 Shape-memory polymers with adjustable high glass transition temperatures *Macromolecules* **48** 3582–9
[18] Xie Q, Fu K, Liang S, Liu B, Lu L, Yang X, Huang Z and Lü F 2018 Micro-structure and thermomechanical properties of crosslinked epoxy composite modified by Nano-SiO_2: a molecular dynamics simulation *Polymers* **10** 801
[19] Wick C D, Peters A J and Li G 2021 Quantifying the contributions of energy storage in a thermoset shape memory polymer with high stress recovery: a molecular dynamics study *Polymer* **213** 123319
[20] Safranski D L and Gall K 2008 Effect of chemical structure and crosslinking density on the thermo-mechanical properties and toughness of (meth)acrylate shape memory polymer networks *Polymer* **49** 4446–55
[21] Hu X, Zhang D and Sheiko S S 2018 Cooling-triggered shapeshifting hydrogels with multi-shape memory performance *Adv. Mater.* **30** 1707461
[22] Xie T 2011 Recent advances in polymer shape memory *Polymer* **52** 4985–5000
[23] Lai H Y, Wang H Q, Lai J C and Li C H 2019 A self-healing and shape memory polymer that functions at body temperature *Molecules* **24** 3224
[24] Leungpuangkaew S, Amornkitbamrung L, Phetnoi N, Sapcharoenkun C, Jubsilp C, Ekgasit S and Rimdusit S 2023 Magnetic- and light-responsive shape memory polymer nanocomposites from bio-based benzoxazine resin and iron oxide nanoparticles *Adv. Ind. Eng. Polym. Res.* **6** 215–25
[25] Jin X, Li X, Liu X, Du L, Su L, Ma Y and Ren S 2023 Simple lignin-based, light-driven shape memory polymers with excellent mechanical properties and wide range of glass transition temperatures *Int. J. Biol. Macromol.* **228** 528–36
[26] Ze Q, Kuang X, Wu S, Wong J, Montgomery S M, Zhang R, Kovitz J M, Yang F, Qi H J and Zhao R 2020 Magnetic shape memory polymers with integrated multifunctional shape manipulation *Adv. Mater.* **32** 1906657
[27] van Vilsteren S J M, Yarmand H and Ghodrat S 2021 Review of magnetic shape memory polymers and magnetic soft materials *Magnetochemistry* **7** 123
[28] Liu Y, Lv H, Lan X, Leng J and Du S 2009 Review of electro-active shape-memory polymer composite *Compos. Sci. Technol.* **69** 2064–8
[29] Zainal M A, Ahmad A and Mohamed Ali M S 2017 Frequency-controlled wireless shape memory polymer microactuator for drug delivery application *Biomed. Microdevices* **19** 8
[30] Li G, Fei G, Xia H, Han J and Zhao Y 2012 Spatial and temporal control of shape memory polymers and simultaneous drug release using high intensity focused ultrasound *J. Mater. Chem.* **22** 7692–6
[31] Bhargava A, Peng K and Shahab S 2019 Dynamics of focused ultrasound actuated shape memory polymers *Proc. SPIE* **10967**
[32] Bhargava A, Peng K, Stieg J, Mirzaeifar R and Shahab S 2017 Ultrasound actuation of shape-memory polymer filaments: acoustic-thermoelastic modeling and testing *ASME 2017*

conf. on smart materials, adaptive structures and intelligent systems (https://doi.org/10.1115/SMASIS2017-3832)
[33] Alvarez V A, Ruscekaite R A and Vazquez A 2003 Mechanical properties and water absorption behavior of composites made from a biodegradable matrix and alkaline-treated sisal fibers *J. Compos. Mater.* **37** 1575–88
[34] Liu B, Xia H, Fei G, Li G and Fan W 2013 High-intensity focused ultrasound-induced thermal effect for solid polymer materials *Macromol. Chem. Phys.* **214** 2519–27
[35] Bruinewoud H Ultrasound-induced drug release from polymer matrices: the glass transition temperature as a thermo-responsive switch Phd Thesis 2 (Research NOT TU/e / Graduation TU/e) Technische Universiteit Eindhoven
[36] Yakacki C M, Shandas R, Lanning C, Rech B, Eckstein A and Gall K 2007 Unconstrained recovery characterization of shape-memory polymer networks for cardiovascular applications *Biomaterials* **28** 2255–63
[37] Gall K, Yakacki C M, Liu Y, Shandas R, Willett N and Anseth K S 2005 Thermomechanics of the shape memory effect in polymers for biomedical applications *J. Biomed. Mater. Res.* A **73A** 339–48
[38] Standard A 2005 ASTM D570: standard test method for water absorption of plastics
[39] Crank J 1979 *The Mathematics of Diffusion* (Oxford University Press)
[40] Kalachandra S and Turner D T 1989 Water sorption of plasticized denture acrylic lining materials *Dent. Mater.* **5** 161–4
[41] Kazemi S, Kiaefar A, Hamidina E and Tajvidi M 2007 Water absorption behavior of composites from sawdust and recycled plastics *J. Reinf. Plast. Compos.* **26** 341–8
[42] Ghi P Y, Hill D J T, Maillet D and Whittaker A K 1997 N.m.r. imaging of the diffusion of water into poly(tetrahydrofurfuryl methacrylate-co-hydroxyethyl methacrylate) *Polymer* **38** 3985–9
[43] Nazemi M K and Valix M 2016 Evaluation of acid diffusion behaviour of amine-cured epoxy coatings by accelerated permeation testing method and prediction of their service life *Prog. Org. Coat.* **97** 307–12
[44] Yang H, Wang Z, Huang Z, He J, Liu Z, Chen Y, Tian L, Huang Q and Liu T 2023 Development and validation of diffusion-controlled model for predicting polycyclic aromatic hydrocarbons from baking-free brick derived from oil—based drilling cuttings *J. Environ. Manage.* **325** 116497
[45] Crank J 1968 *Diffusion in Polymers* ed J Crank and G S Park (Academic Press)
[46] Standard A 2012 ASTM D4065: standard practice for plastics: dynamic mechanical properties: determination and report of procedures
[47] Standard A 2008 ASTM D4440-08: standard test method for plastics: dynamic mechanical properties melt rheology
[48] Kinovea *Kinovea* (available at: www.kinovea.org)
[49] DiMarzio E A 1981 Equilibrium theory of glasses *Ann. New York Acad. Sci.* **371** 1
[50] Ramesh N and Duda J L 2000 Diffusion in polymers below the glass transition temperature: comparison of two approaches based on free volume concepts *Korean J. Chem. Eng.* **17** 310–7
[51] Smith K E, Parks S S, Hyjek M A, Downey S E and Gall K 2009 The effect of the glass transition temperature on the toughness of photopolymerizable (meth)acrylate networks under physiological conditions *Polymer* **50** 5112–23
[52] Abasi S, Davis R, Podstawczyk D A and Guiseppi-Elie A 2019 Distribution of water states within poly(HEMA-co-HPMA)-based hydrogels *Polymer* **185** 121978
[53] Hofer K, Mayer E and Johari G P 1990 Glass-liquid transition of water and ethylene glycol solution in poly(2-hydroxyethyl methacrylate) hydrogel *J. Phys. Chem.* **94** 2689–96
[54] Nakamura K, Hatakeyama T and Hatakeyama H 1983 Relationship between hydrogen bonding and bound water in polyhydroxystyrene derivatives *Polymer* **24** 871–6
[55] Corkhill P H, Jolly A M, Ng C O and Tighe B J 1987 Synthetic hydrogels: 1. Hydroxyalkyl acrylate and methacrylate copolymers—water binding studies *Polymer* **28** 1758–66
[56] Morita S 2014 Hydrogen-bonds structure in poly(2-hydroxyethyl methacrylate) studied by temperature-dependent infrared spectroscopy *Front. Chem.* **2** 10
[57] Miller D A 1995 *The Ionic Conductivity of P(2-hydroxyethyl Methacrylate) Hydrogels* (University of Adelaide)
[58] Schissel S M and Jessop J L P 2019 Enhancing epoxide kinetics and tuning polymer properties using hydroxyl-containing (meth)acrylates in hybrid photopolymerizations *Polymer* **161** 78–91
[59] Bulmus V, Chan Y, Nguyen Q and Tran H L 2007 Synthesis and characterization of degradable p(HEMA) microgels: use of acid-labile crosslinkers *Macromol. Biosci.* **7** 446–55
[60] Uthaman A, Xian G, Thomas S, Wang Y, Zheng Q and Liu X 2020 Durability of an epoxy resin and its carbon fiber-reinforced polymer composite upon immersion in water, acidic, and alkaline solutions *Polymers* **12** 614
[61] Huang W M, Yang B, An L, Li C and Chan Y S 2005 Water-driven programmable polyurethane shape memory polymer: demonstration and mechanism *Appl. Phys. Lett.* **86** 114105
[62] Yu Y-J, Hearon K, Wilson T S and Maitland D J 2011 The effect of moisture absorption on the physical properties of polyurethane shape memory polymer foams *Smart Mater. Struct.* **20** 085010
[63] Xiao R and Nguyen T D 2013 Modeling the solvent-induced shape-memory behavior of glassy polymers *Soft Matter* **9** 9455–64
[64] Adam G and Gibbs J H 2004 On the temperature dependence of cooperative relaxation properties in glass-forming liquids *J. Chem. Phys.* **43** 139–46
[65] Chow T S 1980 Molecular interpretation of the glass transition temperature of polymer-diluent systems *Macromolecules* **13** 362–4
[66] Smith K E, Temenoff J S and Gall K 2009 On the toughness of photopolymerizable (meth)acrylate networks for biomedical applications *J. Appl. Polym. Sci.* **114** 2711–22
[67] Lakhera N, Laursen C M, Safranski D L and Frick C P 2012 Biodegradable thermoset shape-memory polymer developed from poly(β-amino ester) networks *J. Polym. Sci.* B **50** 777–89
[68] Yang B, Huang W M, Li C, Lee C M and Li L 2004 On the effects of moisture in a polyurethane shape memory polymer *Smart Mater. Struct.* **13** 191
[69] Aarushi B, Kaiyuan P, Reza M and Shima S 2018 Ultrasound actuated shape-memory polymer based drug delivery containers *Proc. SPIE* **10595**
[70] Rozanova-Pierrat A 2006 Mathematical analysis of Khokhlov-Zabolotskaya-Kuznetsov (KZK) equation
[71] Hamilton M F and Blackstock D T 1998 *Nonlinear Acoustics* illustrated (Academic Press)
[72] Bhargava A 2020 *Dynamics of Smart Materials in High Intensity Focused Ultrasound Field* (Virginia Tech)
[73] Peng K, Shahab S and Mirzaeifar R 2020 Interaction of high-intensity focused ultrasound with polymers at the atomistic scale *Nanotechnology* **32** 045707
[74] Parker N G, Mather M L, Morgan S P and Povey M J 2010 Longitudinal acoustic properties of poly(lactic acid) and poly(lactic-co-glycolic acid) *Biomed. Mater.* **5** 055004